

1 Age differences in head motion and estimates of cortical morphology

2 Christopher R. Madan

3 School of Psychology

4 University of Nottingham

5 Nottingham, United Kingdom

6

7 Corresponding author:

8 Christopher R. Madan

9 School of Psychology, University of Nottingham

10 Nottingham, NG7 2RD, United Kingdom

11 christopher.madan@nottingham.ac.uk

12 Abstract

13 Cortical morphology is known to differ with age, as measured by cortical thickness,
14 fractal dimensionality, and gyrification. However, head motion during MRI scanning
15 has been shown to influence estimates of cortical thickness as well as increase with age.
16 Studies have also found task-related differences in head motion and relationships
17 between body-mass index (BMI) and head motion. Here I replicated these prior
18 findings, as well as several others, within a large, open-access dataset (Centre for
19 Ageing and Neuroscience, CamCAN). This is a larger dataset than these results have
20 been demonstrated previously, within a sample size of more than 600 adults across the
21 adult lifespan. While replicating prior findings is important, demonstrating these key
22 findings concurrently also provides an opportunity for additional related analyses:
23 Critically, I test for the influence of head motion on cortical fractal dimensionality and
24 gyrification; effects were statistically significant in some cases, but small in magnitude.

25 Age differences in head motion and estimates of cortical morphology

26 **1 Introduction**

27 Head motion during the acquisition of magnetic resonance imaging (MRI) can lead to
28 artifacts when estimating brain activity and structure. With functional MRI (fMRI),
29 volumes are acquired relatively quickly—often every 1-3 seconds—allowing for the
30 estimation and correction of head motion artifacts. Using innovative techniques such
31 as prospective motion correction (Dosenbach et al., 2017; Federau & Gallichan, 2016;
32 Maclaren et al., 2013; Stucht et al., 2015; Tisdall et al., 2016) and custom-designed,
33 individualized head-cases (<https://caseforge.co>), effects of head motion can be
34 attenuated. However, these solutions are not suitable for large studies of
35 inter-individual differences in brain morphology where changes to the MRI scan
36 sequence or custom-built equipment for each participant are often not practical. In the
37 current study, I assessed relationships between age and body-mass index (BMI) on
38 head motion, task-related differences in head motion, and the influence of head motion
39 on estimates of cortical morphology. In light of these findings, many of which are
40 replications, I propose a potential method for attenuating head motion during
41 structural MRIs, as well as discuss limitations of this method.

42 Prior studies have demonstrated that older adults tend to have more head motion
43 than younger adults (Andrews-Hanna et al., 2007; Chan et al., 2014; Savalia et al., 2017;
44 Pardoe et al., 2016). Unfortunately, other studies have also shown that head motion can
45 lead to lower cortical thickness estimates (Alexander-Bloch et al., 2016; Pardoe et al.,
46 2016; Reuter et al., 2015; Savalia et al., 2017), as such, age-related differences in cortical
47 thickness (e.g., Fjell et al., 2009; McKay et al., 2014; Salat et al., 2004) may be
48 exaggerated by age-related differences in head motion. In addition to age, obesity has
49 also been associated with head motion (Beyer et al., 2017; Hodgson et al., 2017). In
50 particular, these associations have been shown with respect to body-mass index (BMI;
51 kg/m^2), which is measured as body weight (in kg) divided by body height (in m)
52 squared—despite the relatively coarse nature of BMI (e.g., does not differentiate

53 between muscle vs. fat mass) (Diverse Populations Collaborative Group, 2005;
54 Romero-Corral et al., 2008). Findings of relationships between obesity and cortical
55 thickness have been mixed (Shaw et al., 2017, 2018; Veit et al., 2014). More generally,
56 head motion has been suggested to be a neurobiological trait—being both stable over
57 time and heritable (Engelhardt et al., 2017; Hodgson et al., 2017; Zeng et al., 2014).

58 There is also evidence that fMRI tasks can differ in the degree of associated head
59 motion (Alexander et al., 2017; Huijbers et al., 2017; Greene et al., 2018; Vanderwal et
60 al., 2015; Wylie et al., 2014; Yuan et al., 2009). With this in mind, it may be beneficial to
61 present participants with a task to attend to *during structural scans*, with the objective of
62 decreasing head motion; typically structural scans are accompanied by the presentation
63 of a blank screen or otherwise lack of instruction of attending to a visual stimulus.

64 Madan and Kensinger (2016) showed that a structural metric, fractal
65 dimensionality (FD), may be more sensitive to age-related differences in cortical
66 structure than cortical thickness (also see Madan & Kensinger, 2018). In a preliminary
67 analysis to examine the influence of head motion on age-related differences in cortical
68 fractal dimensionality, Madan and Kensinger (2016) showed qualitative evidence of
69 age-related differences in fractal dimensionality in a small sample ($N = 7$) of
70 post-mortem MRIs. However, as this sample was small and also less indicative of
71 potential head motion effects in *in vivo* MR imaging, further work is necessary. To more
72 directly test for the additive influence of head motion on estimates of cortical
73 morphology, beyond aging, here I also tested for a relationship of fMRI-estimated head
74 motion on cortical fractal dimensionality, as well as on mean cortical thickness.
75 Additionally, as recent studies have found that gyrification also decreases with age
76 (Cao et al., 2017; Hogstrom et al., 2013; Madan & Kensinger, 2016, 2018), it was also
77 included in the analysis presented here. Test-retest reliability of estimates for these
78 structural measures has recently been compared (Madan & Kensinger, 2017b), but
79 robustness to head motion has yet to be assessed.

80 Using the rich, open-access dataset from Cambridge Centre for Ageing and
81 Neuroscience (CamCAN) (Shafto et al., 2014; Taylor et al., 2017), here I sought to

82 replicate these myriad of prior findings, as well as test for influences of head motion on
83 fractal dimensionality and gyrification.

84 **2 Methods**

85 **2.1 Dataset**

86 Data used in the preparation of this work were obtained from the Cambridge Centre
87 for Ageing and Neuroscience (CamCAN) repository, available at
88 <http://www.mrc-cbu.cam.ac.uk/datasets/camcan/> (Shafto et al., 2014;
89 Taylor et al., 2017). The CamCAN dataset includes structural and functional MRI data
90 for a sample of 648 adults across the adult lifespan (aged 18-88; Mean (SD)
91 = 54.2 (18.5)). All participants were cognitively healthy (MMSE > 24) and were free of
92 any neurological or serious psychiatric conditions. See Taylor et al. (2017) for
93 additional details about the sample.

94 A total of 8 participants were excluded from further analyses due to problems
95 with cortical reconstruction or gyrification estimation, yielding a final sample size of
96 640 adults (326 female, 314 male). Height and weight measurements were available for
97 559 of the 648 participants (280 female, 279 male), additionally allowing for the
98 calculation of body-mass index (BMI) for this subset of participants (also see Ronan et
99 al., 2016).

100 Structural measures are derived from a T1-weighted volume acquired using a 3 T
101 Siemens Trio MRI scanner with an MPRAGE sequence. Scan parameters were as
102 follows: TR = 2250 ms, TE = 2.99 ms, flip angle = 9°, voxel size = 1 × 1 × 1 mm,
103 GRAPPA = 2, TI = 900 ms. Head motion was primarily estimated from two fMRI scans,
104 during rest and a movie-watching task. Both scans lasted for 8 min and 40 s (i.e., 520 s
105 total). For the rest scan, participants were instructed to rest with their eyes closed. For
106 the movie scan, participants watched and listened to condensed version of Alfred
107 Hitchcock's (1961) "Bang! You're Dead" (Campbell et al., 2015; Hasson et al., 2008).
108 Note that different scan sequences were used for both of these scans, with volumes

109 collected every 1.970 s or 2.470 s for the rest and movie scans, respectively (see Taylor
110 et al., 2017, for more details); both rest and movie scans had the same voxel size,
111 $3 \times 3 \times 4.44$ mm (32 axial slices, 3.7 mm thick, 0.74 mm gap).

112 **2.2 Preprocessing of the structural MRI data**

113 The T1-weighted structural MRIs were processed using FreeSurfer v6.0
114 (<https://surfer.nmr.mgh.harvard.edu/>) (Dale et al., 1999; Fischl, 2012; Fischl
115 & Dale, 2000). Surface meshes and cortical thickness was estimated using the standard
116 processing pipeline, i.e., `recon-all`, and no manual edits were made to the surfaces.
117 Gyrfication was calculated using FreeSurfer, as described in Schaer et al. (2012).

118 Fractal dimensionality (FD) is a measure of the complexity of a structure and has
119 previously been shown to decrease in relation to aging for cortical (Madan & Kensinger,
120 2016, 2018) and subcortical (Madan & Kensinger, 2017a; Madan, 2018) structures and
121 has been shown to have high test-retest reliability (Madan & Kensinger, 2017b). FD
122 was calculated using the calcFD toolbox (<http://cmadan.github.io/calcFD/>)
123 (Madan & Kensinger, 2016) using the dilation method and filled structures (denoted as
124 FD_f in prior studies). Briefly, FD measures the effective dimensionality of a structure
125 by counting how many grid ‘boxes’ of a particular size are needed to contain a
126 structure; these counts are then contrasted relative to the box sizes in log-space,
127 yielding a scale-invariant measure of the complexity of a structure. This is
128 mathematically calculated as $FD = -\Delta \log_2(\text{Count}) / \Delta \log_2(\text{Size})$, where Size was set
129 to $\{1, 2, 4, 8, 16\}$ (i.e., powers of 2, ranging from 0 to 4). To correct for the variability in
130 FD estimates associated with the alignment of the box-grid with the structure, a
131 dilation algorithm was used which instead relies on a 3D-convolution operation
132 (`convn` in MATLAB) as this approach yields to more reliable estimates of FD. This
133 computational issue is described mathematical and demonstrated in simulations in
134 Madan and Kensinger (2016), and empirically shown in Madan and Kensinger (2017b).
135 See Madan and Kensinger (2016, 2018) for additional background on fractal
136 dimensionality and its application to brain imaging data.

137 **2.3 Estimates of head motion**

138 Head motion was estimated using two approaches:

139 (1) Measured as the frame-wise displacement using the three translational and
140 three rotational realignment parameters. Realignment parameters were included as
141 part of the preprocessed fMRI data (Taylor et al., 2017), in the form of the `rp_*.txt`
142 output generated by SPM realign procedure. Rotational displacements were converted
143 from degrees to millimeters by calculating the displacement on the surface of a sphere
144 with a radius of 50 mm (as in Power et al., 2012). Frame-wise displacement was
145 substantially higher between volumes at the beginning of each scan run, so the first
146 five volumes were excluded. This is the same approach to estimating head motion that
147 is commonly used (e.g., Alexander-Bloch et al., 2016; Engelhardt et al., 2017; Power et
148 al., 2012; Savalia et al., 2017).

149 (2) Estimated directly from the T1-weighted volume as ‘average edge strength’
150 (AES) (Aksoy et al., 2012; Zacà et al., in press). This approach measures the intensity of
151 contrast at edges within an image. Higher AES values correspond to less motion, with
152 image blurring yielding decreased tissue contrast and lower AES values. AES was
153 calculated using the toolbox provided by Zacà et al. (in press), on the skull-stripped
154 volumes generated as an intermediate stage of the FreeSurfer processing pipeline. AES
155 is calculated on two-dimensional image planes and was performed on each plane
156 orientation (axial, sagittal, and coronal).

157 **2.4 Model comparison approach**

158 Effects of head motion on estimates of cortical morphology (thickness, fractal
159 dimensionality, and gyrification) were assessed using a hierarchical regression
160 procedure using MATLAB. Age was first input, followed by BMI (both with and
161 without age), followed by estimates of head motion from each fMRI scan and the
162 related interaction term with age. In total, eight models were examined, as listed in
163 Table1. Model fitness was assessed using both R^2 and ΔBIC .

164 Bayesian Information Criterion, BIC , is a model fitness index that includes a

165 penalty based on the number of free parameters (Schwarz, 1978). Smaller *BIC* values
166 correspond to better model fits. By convention, two models are considered equivalent
167 if $\Delta BIC < 2$ (Burnham & Anderson, 2004). As *BIC* values are based on the relevant
168 dependent variable, ΔBIC values are reported relative to the best-performing model
169 (i.e., $\Delta BIC = 0$ for the best model considered).

170 **3 Results**

171 **3.1 fMRI-estimated head motion**

172 As shown in Figure 1, older adults had increased head motion relative to younger
173 adults in both the rest and movie scans [rest: $r(638) = .351, p < .001$; movie:
174 $r(638) = .430, p < .001$]. Head motion was also greater in the rest scan than during the
175 movie watching [$t(639) = 23.35, p < .001$, Cohen's $d = 0.99, M_{diff} = 1.528$ mm/min].
176 Nonetheless, head motion was correlated between the fMRI scans [$r(638) = .484,$
177 $p < .001$]. While this correlation between scans is expected, particularly since both
178 were collected in the same MRI session, studies have provided evidence that head
179 motion during scanning may be a trait (Engelhardt et al., 2017; Hodgson et al., 2017;
180 Zeng et al., 2014). Moreover, this correlation provides additional evidence that motion
181 during the fMRI scans is consistently larger in some individuals than others,
182 suggesting it similarly affected the structural scans more for some individuals than
183 others and appropriate to include as a predictor for the cortical morphology estimates.

184 As expected based on prior literature (Beyer et al., 2017; Hodgson et al., 2017),
185 head motion was also correlated with body-mass index (BMI) [rest: $r(557) = .456,$
186 $p < .001$; movie: $r(557) = .335, p < .001$] (Figure 1). While BMI was also correlated with
187 age [$r(557) = .274, p < .001$], BMI-effects on head motion persisted after accounting for
188 age differences [rest: $r_p(555) = .340, p < .001$; movie: $r_p(555) = .249, p < .001$].

189 While head motion was substantially lower in the movie condition than during
190 rest, it was relatively stable over time (e.g., it does not tend to decrease over time).
191 However, in the movie watching task, there is evidence of systematic stimuli-evoked

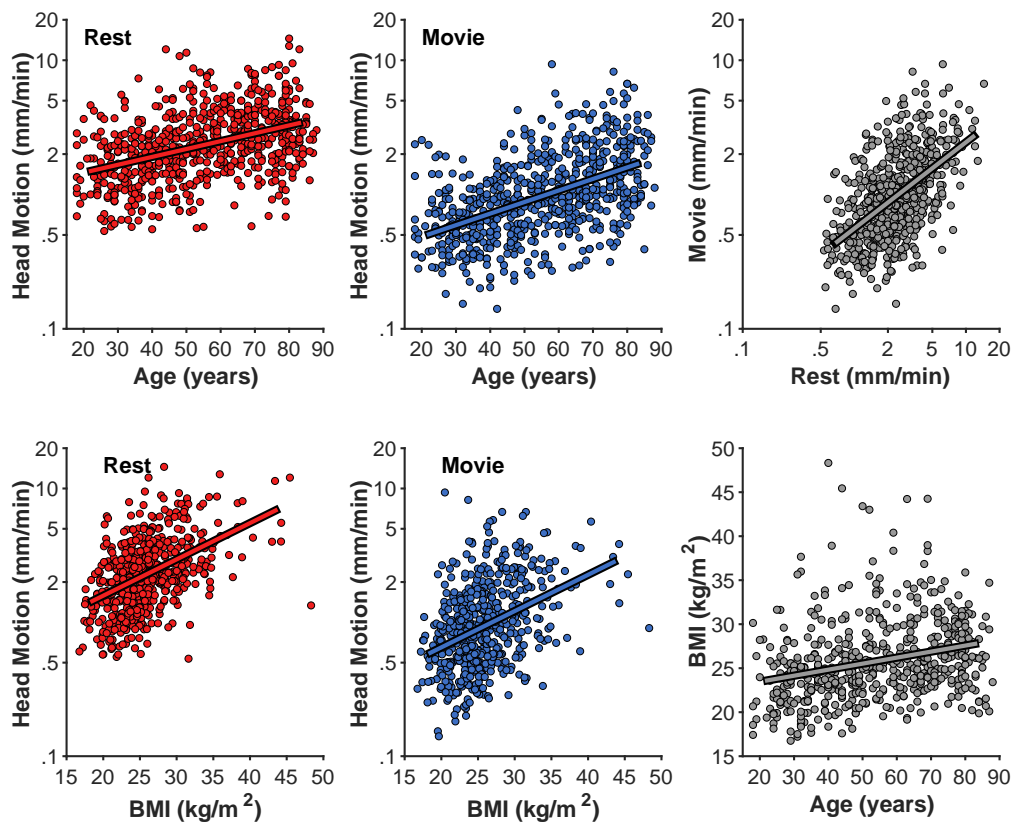


Figure 1. Age-related differences in head motion. Correlations between average head motion (mm/min) with age and body-mass index (BMI) for the rest and movie fMRI scans, between fMRI scans, and between age and BMI. Head motion axes are log-10 scaled to better show inter-individual variability.

192 increases in head motion (Figure 2), e.g., around 280 s and 360 s. These periods of
193 increased head motion correspond to events within the movie; in the first period the
194 boy is loading the real gun with bullets, the second, more prominent period is a
195 suspenseful scene where it appears that the boy may accidentally shoot someone.
196 Moreover, these events also correspond to fMRI differences in attentional control and
197 inter-subject synchrony (see Campbell et al., 2015).

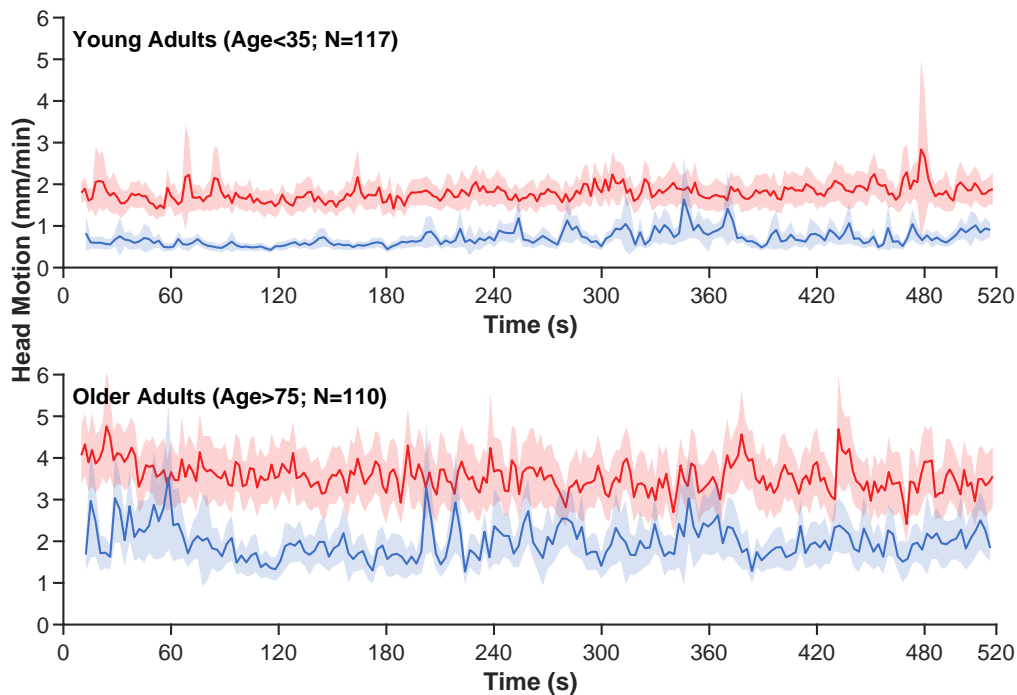


Figure 2. Averaged time-course of head motion for rest (red) and movie (blue) fMRI scans for young and older adults. Bands represent 95% confidence intervals.

198 3.2 T1-estimated head motion

199 Head motion was also estimated directly from the T1-weighted volume as the average
200 edge strength (AES), following from Zacà et al. (in press); higher AES values
201 correspond to less motion. Based on the T1 acquisition parameters, AES in the axial
202 plane orientation should be the most affected by head motion; nonetheless, I calculated
203 AES for each plane orientation. AES in the axial and sagittal planes was moderately
204 related to age [axial: $r(639) = .493, p < .001$; sagittal: $r(639) = .525, p < .001$] (Figure 3);
205 AES in the coronal was only weakly correlated with age [$r(639) = -.131, p < .001$].
206 AES in the axial and sagittal planes were strongly correlated with each other
207 [$r(639) = .702, p < .001$].

208 Interestingly, AES was relatively not related to BMI [all $|r|$'s $< .2$]. AES was also
209 relatively unrelated to fMRI-estimated head motion [rest: $r(639) = .112, p = .005$;
210 movie: $r(639) = .148, p < .001$]. Thus, while AES is sensitive to an MR image property
211 related to age, it seems to be distinct from fMRI-estimated head motion. A likely

212 possibility is tht AES here is detecting age-related differences in gray/white matter
213 contrast ratio (GWR), as have been previously observed (Knight et al., 2016; Magnaldi
214 et al., 1993; Salat et al., 2009).

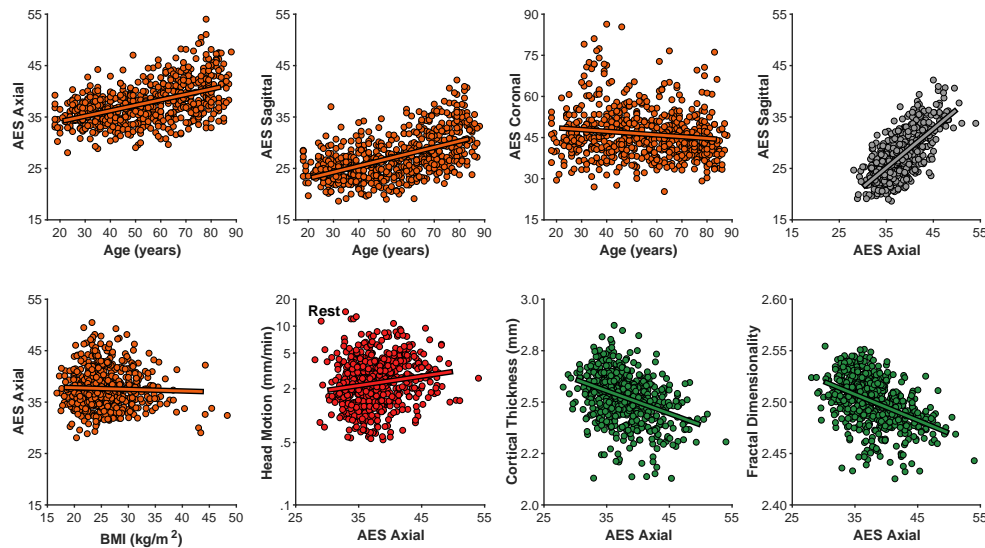


Figure 3. Relationships between motion estimated from the structural volume using average edge strength (AES) in different planes with age, BMI, rest-fMRI estimated motion, cortical thickness, and fractal dimensionality.

215 3.3 Cortical morphology

216 As shown in Figure 4, mean cortical thickness significantly decreased with age
217 [$r(638) = -.652, p < .001, -0.0432$ mm/decade], as did fractal dimensionality
218 [$r(638) = -.705, p < .001, -0.0097$ FD_f /decade] and gyrification [$r(638) = -.427,$
219 $p < .001, -0.0372$ GI /decade]. All three slopes (change in metric per decade) are
220 nearly identical to those first calculated by Madan and Kensinger (2016), as is the
221 general finding of higher age-related differences in fractal dimensionality and weaker
222 differences in gyrification (also see Madan & Kensinger, 2018). However, it is also
223 worth acknowledging that AES in the axial and sagittal planes were comparably
224 correlated with age as gyrification. Effects of BMI on all three measures of cortical
225 morphology were relatively weak [thickness: $r(557) = -.169, p < .001$; fractal

226 dimensionality: $r(557) = -.168, p < .001$; gyrification $r(557) = -.083, p = .049$].

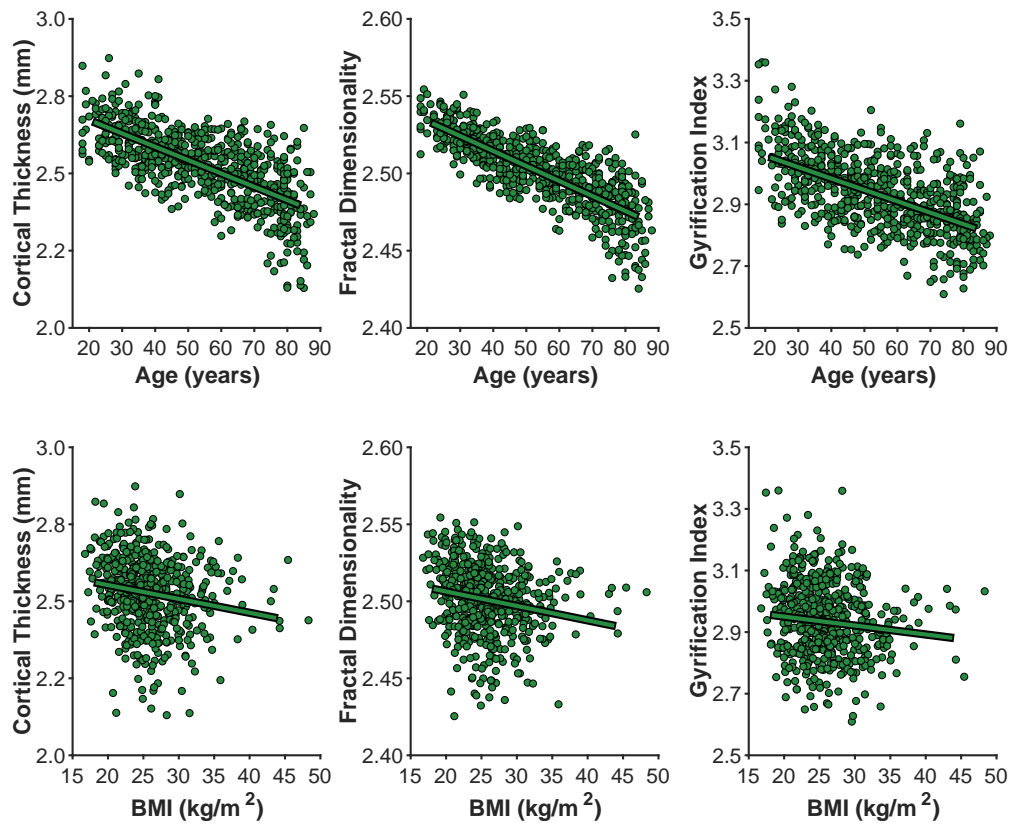


Figure 4. Age- and BMI-related differences in the three cortical morphology measures examined here: thickness, fractal dimensionality, and gyrification.

227 Of particular interest, I examined the influence of head motion on the cortical
228 morphology estimates. For all three measures, head motion explained only a small
229 amount of additional variance beyond age, as shown in Table 1. Nonetheless, head
230 motion from the movie scan did explain significant additional variance, as measured
231 by Δ BIC, however, this only accounted for an additional 1% variance in the cortical
232 morphology measures. In the model of cortical thickness including head motion from
233 the movie scan (but not the interaction), age related changes corresponded to -0.0398
234 mm/decade, while head motion contributed -0.0135 mm/(mm/min).

Model	Predictors	Thickness		FD		Gyrification	
		R^2	ΔBIC	R^2	ΔBIC	R^2	ΔBIC
1	Age	.425	6.98	.497	3.15	.192	3.65
2	BMI	.029	455.85	.028	805.25	.007	243.17
3	Age + BMI	.425	168.82	.487	454.69	.183	140.23
4	Age + Movement(Rest)	.429	10.01	.500	5.65	.192	10.07
5	Age + Movement(Movie)	.437	0.00	.504	0.00	.194	8.44
6	Age + Movement(Movie) + Age×Movement(Movie)	.427	11.64	.499	6.58	.205	0.00
7	Age + AES(axial)	.443	0.23	.507	3.18	.194	14.83
8	Age + AES(axial) + Age×AES(axial)	.428	17.58	.500	12.42	.208	3.76

Table 1

Variance explained and model fits of cortical measures by age, BMI, and head motion estimates. Note that R^2 decreases after the inclusion of BMI as models 2 and 3 can only be calculated on a subset of participants (559 out of 640 participants) since height and weight information was not available for all participants.

235 4 Discussion

236 In the current study, I replicated several prior findings as well as tested for a few novel
237 effects of head motion. First I outline the key findings of prior studies that were
238 replicated here:

- 239 (1) Increased head motion in older adults (replicating Savalia et al., 2017; Pardoe et
240 al., 2016).
- 241 (2) BMI is correlated with head motion (replicating Beyer et al., 2017; Hodgson et al.,
242 2017).
- 243 (3) Less head motion occurs when watching a movie than during rest (replicating
244 Vanderwal et al., 2015; Huijbers et al., 2017).
- 245 (4) Head motion in different scans from the same individuals is correlated and
246 indexes reliable inter-individual differences (replicating Zeng et al., 2014;
247 Engelhardt et al., 2017; Hodgson et al., 2017).
- 248 (5) Cortical thickness decreases with age (replicating Fjell et al., 2009; Salat et al.,
249 2004).

250 (6) Fractal dimensionality and gyrification also decrease with age (replicating Madan
251 & Kensinger, 2016, 2018; Hogstrom et al., 2013).

252 (7) More head motion leads to lower estimates of cortical thickness (replicating
253 Reuter et al., 2015; Savalia et al., 2017).

254

255 In addition to these replications, the new findings were:

256 (8) Head motion leads to nominally lower estimates of fractal dimensionality and
257 gyrification.

258 (9) Head motion estimated from the structural volume itself (i.e., average edge
259 strength [AES]) correlated with age, but not BMI.

260 (10) AES may be sensitive to gray/white matter contrast ratio (GWR).

261 (11) AES was only weakly related to fMRI-measured head motion.

262 (12) Global cortical morphology is not related to BMI.

263 Likely most important, I found significantly more movement during resting state
264 than watching a movie, but are quite correlated still (replicating the findings of
265 Huijbers et al., 2017; Greene et al., 2018). Based on this evidence, I would recommend
266 that participants be given movie-watching task *during structural scans* to reduce
267 movement during these longer volume acquisitions and improve scan quality.
268 Suggestions of potential systematic increases in head motion, however, suggest that
269 less eventful movie content may be preferable for both maintaining participants'
270 attention and minimizing movement-based reactions (e.g., see Vanderwal et al., 2015).
271 While this approach is not common, it has been used in some recent large-scale studies,
272 such as the Human Connectome Project (HCP) (Marcus et al., 2013) and Adolescent
273 Brain Cognitive Development (ABCD) study (Casey et al., in press), and has also been
274 suggested and used elsewhere, particularly in MRI studies with children (Greene et al.,
275 2016; Bellis et al., 2001; Howell et al., in press; Overmeyer, 1996; Pliszka et al., 2006;
276 Raschle et al., 2009; Theys et al., 2014; von Rhein et al., 2015; Wu Nordahl et al., 2008).

277 However, it is also important to consider the context that this movie watching would
278 occur in. For instance, if the structural scan is followed by a resting-state fMRI scan,
279 cognitive processes related to the movie watching will ‘spill over’ and influence
280 patterns of brain activity in a subsequent rest period (e.g., Tambini & Davachi, 2013;
281 van Kesteren et al., 2010; Eryilmaz et al., 2011).

282 Estimates of cortical thickness were significantly influenced by head motion
283 (replicating Savalia et al., 2017; Reuter et al., 2015), though the influence of this
284 appeared to be relatively small. Effects of head motion on fractal dimensionality were
285 also significant, but even smaller in magnitude, while head motion did not
286 significantly influence estimates of gyrification. The results here also served as a
287 replication age-related differences in fractal dimensionality and gyrification (Madan &
288 Kensinger, 2016, 2018).

289 Interestingly, average edge strength (AES) did not correlate well with fMRI
290 motion, but did correlate with age. This may be related to age-related differences in
291 gray/white matter contrast ratio (GWR), as AES corresponds to the degree of tissue
292 intensity contrast. This finding may be important when examining differences in AES
293 between different samples (e.g., patients vs. controls).

294 While the results here are predominately replications of prior work, they
295 nonetheless integrate the key findings of several papers through a single, open-access
296 dataset, that also has a larger sample size than these previous studies. Moreover, these
297 results serve as an example to highlight the benefits of open data sharing on improving
298 our understanding of brain morphology (see Madan, 2017, for a detailed discussion).

299 **5 Conclusion**

300 Head motion influences estimates of cortical morphology, but can be attenuated by
301 using an engaging task, such as movie watching, rather than merely instructing
302 participants to rest. Decreasing head motion is particularly important when studying
303 aging populations, where head motion is greater than for young adults, but
304 considerations are necessary to see how this may ‘carry over’ and influence a

305 subsequent scan, such as resting-state fMRI.

306 **Acknowledgments**

307 Data collection and sharing for this project was provided by the Cambridge Centre for
308 Ageing and Neuroscience (CamCAN). CamCAN funding was provided by the UK
309 Biotechnology and Biological Sciences Research Council (BBSRC) (BB/H008217/1),
310 together with support from the UK Medical Research Council (MRC) and the
311 University of Cambridge.

312 I would like to thank Darren Price and Rogier Kievit for assistance with accessing
313 the CamCAN data. I would also like to thank Jordan Theriault and Alexis Porter for
314 insightful discussions.

References

315

- 316 Aksoy, M., Forman, C., Straka, M., Çukur, T., Hornegger, J., & Bammer, R. (2012).
317 Hybrid prospective and retrospective head motion correction to mitigate
318 cross-calibration errors. *Magnetic Resonance in Medicine*, *67*, 1237–1251. doi:
319 10.1002/mrm.23101
- 320 Alexander, L. M., Escalera, J., Ai, L., Andreotti, C., Febre, K., Mangone, A., ... Milham,
321 M. P. (2017). An open resource for transdiagnostic research in pediatric mental
322 health and learning disorders. *Scientific Data*, *4*, 170181. doi:
323 10.1038/sdata.2017.181
- 324 Alexander-Bloch, A., Clasen, L., Stockman, M., Ronan, L., Lalonde, F., Giedd, J., &
325 Raznahan, A. (2016). Subtle in-scanner motion biases automated measurement of
326 brain anatomy from in vivo MRI. *Human Brain Mapping*, *37*, 2385–2397. doi:
327 10.1002/hbm.23180
- 328 Andrews-Hanna, J. R., Snyder, A. Z., Vincent, J. L., Lustig, C., Head, D., Raichle, M. E.,
329 & Buckner, R. L. (2007). Disruption of large-scale brain systems in advanced
330 aging. *Neuron*, *56*, 924–935. doi: 10.1016/j.neuron.2007.10.038
- 331 Bellis, M. D. D., Keshavan, M. S., Beers, S. R., Hall, J., Frustaci, K., Masalehdan, A., ...
332 Boring, A. M. (2001). Sex differences in brain maturation during childhood and
333 adolescence. *Cerebral Cortex*, *11*, 552–557. doi: 10.1093/cercor/11.6.552
- 334 Beyer, F., Masouleh, S. K., Huntenburg, J. M., Lampe, L., Luck, T., Riedel-Heller, S. G.,
335 ... Witte, A. V. (2017). Higher body mass index is associated with reduced
336 posterior default mode connectivity in older adults. *Human Brain Mapping*, *38*,
337 3502–3515. doi: 10.1002/hbm.23605
- 338 Burnham, K. P., & Anderson, D. R. (2004). Multimodel inference. *Sociological Methods &*
339 *Research*, *33*, 261–304. doi: 10.1177/0049124104268644
- 340 Campbell, K. L., Shafto, M. A., Wright, P., Tsvetanov, K. A., Geerligs, L., Cusack, R., ...
341 Villis, L. (2015). Idiosyncratic responding during movie-watching predicted by
342 age differences in attentional control. *Neurobiology of Aging*, *36*, 3045–3055. doi:
343 10.1016/j.neurobiolaging.2015.07.028

- 344 Cao, B., Mwangi, B., Passos, I. C., Wu, M.-J., Keser, Z., Zunta-Soares, G. B., ... Soares,
345 J. C. (2017). Lifespan gyrification trajectories of human brain in healthy
346 individuals and patients with major psychiatric disorders. *Scientific Reports*, 7.
347 doi: 10.1038/s41598-017-00582-1
- 348 Casey, B., Cannonier, T., Conley, M. I., Cohen, A. O., Barch, D. M., Heitzeg, M. M., ...
349 Dale, A. M. (in press). The Adolescent Brain Cognitive Development (ABCD)
350 study: Imaging acquisition across 21 sites. *Developmental Cognitive Neuroscience*.
351 doi: 10.1016/j.dcn.2018.03.001
- 352 Chan, M. Y., Park, D. C., Savalia, N. K., Petersen, S. E., & Wig, G. S. (2014). Decreased
353 segregation of brain systems across the healthy adult lifespan. *Proceedings of the*
354 *National Academy of Sciences USA*, 111, E4997–E5006. doi:
355 10.1073/pnas.1415122111
- 356 Dale, A. M., Fischl, B., & Sereno, M. I. (1999). Cortical surface-based analysis: I.
357 segmentation and surface reconstruction. *NeuroImage*, 9, 179–194. doi:
358 10.1006/nimg.1998.0395
- 359 Diverse Populations Collaborative Group. (2005). Weight-height relationships and
360 body mass index: Some observations from the diverse populations collaboration.
361 *American Journal of Physical Anthropology*, 128, 220–229. doi: 10.1002/ajpa.20107
- 362 Dosenbach, N. U., Koller, J. M., Earl, E. A., Miranda-Dominguez, O., Klein, R. L., Van,
363 A. N., ... Fair, D. A. (2017). Real-time motion analytics during brain MRI
364 improve data quality and reduce costs. *NeuroImage*, 161, 80–93. doi:
365 10.1016/j.neuroimage.2017.08.025
- 366 Engelhardt, L. E., Roe, M. A., Juranek, J., DeMaster, D., Harden, K. P., Tucker-Drob,
367 E. M., & Church, J. A. (2017). Children's head motion during fMRI tasks is
368 heritable and stable over time. *Developmental Cognitive Neuroscience*, 25, 58–68.
369 doi: 10.1016/j.dcn.2017.01.011
- 370 Eryilmaz, H., Ville, D. V. D., Schwartz, S., & Vuilleumier, P. (2011). Impact of transient
371 emotions on functional connectivity during subsequent resting state: A wavelet
372 correlation approach. *NeuroImage*, 54, 2481–2491. doi:

- 373 10.1016/j.neuroimage.2010.10.021
- 374 Federau, C., & Gallichan, D. (2016). Motion-correction enabled ultra-high resolution
375 In-Vivo 7 T-MRI of the brain. *PLOS ONE*, *11*, e0154974. doi:
376 10.1371/journal.pone.0154974
- 377 Fischl, B. (2012). FreeSurfer. *NeuroImage*, *62*, 774–781. doi:
378 10.1016/j.neuroimage.2012.01.021
- 379 Fischl, B., & Dale, A. M. (2000). Measuring the thickness of the human cerebral cortex
380 from magnetic resonance images. *Proceedings of the National Academy of Sciences*
381 *USA*, *97*, 11050–11055. doi: 10.1073/pnas.200033797
- 382 Fjell, A. M., Westlye, L. T., Amlien, I., Espeseth, T., Reinvang, I., Raz, N., ... Walhovd,
383 K. B. (2009). High consistency of regional cortical thinning in aging across
384 multiple samples. *Cerebral Cortex*, *19*, 2001–2012. doi: 10.1093/cercor/bhn232
- 385 Greene, D. J., Black, K. J., & Schlaggar, B. L. (2016). Considerations for MRI study
386 design and implementation in pediatric and clinical populations. *Developmental*
387 *Cognitive Neuroscience*, *18*, 101–112. doi: 10.1016/j.dcn.2015.12.005
- 388 Greene, D. J., Koller, J. M., Hampton, J. M., Wesevich, V., Van, A. N., Nguyen, A. L., ...
389 Dosenbach, N. U. (2018). Behavioral interventions for reducing head motion
390 during MRI scans in children. *NeuroImage*, *171*, 234–245. doi:
391 10.1016/j.neuroimage.2018.01.023
- 392 Hasson, U., Landesman, O., Knappmeyer, B., Vallines, I., Rubin, N., & Heeger, D. J.
393 (2008). Neurocinematics: The neuroscience of film. *Projections*, *2*, 1–26. doi:
394 10.3167/proj.2008.020102
- 395 Hitchcock, A. (1961). *Bang! You're Dead [Motion Picture]*. Hollywood: Shamley
396 Productions.
- 397 Hodgson, K., Poldrack, R. A., Curran, J. E., Knowles, E. E., Mathias, S., Göring, H. H.,
398 ... Glahn, D. C. (2017). Shared genetic factors influence head motion during MRI
399 and body mass index. *Cerebral Cortex*, *27*, 5539–5546. doi: 10.1093/cercor/bhw321
- 400
- 401 Hogstrom, L. J., Westlye, L. T., Walhovd, K. B., & Fjell, A. M. (2013). The structure of the

- 402 cerebral cortex across adult life: Age-related patterns of surface area, thickness,
403 and gyrification. *Cerebral Cortex*, 23, 2521–2530. doi: 10.1093/cercor/bhs231
- 404 Howell, B. R., Styner, M. A., Gao, W., Yap, P.-T., Wang, L., Baluyot, K., ... Elison, J. T.
405 (in press). The UNC/UMN baby connectome project (BCP): An overview of the
406 study design and protocol development. *NeuroImage*. doi:
407 10.1016/j.neuroimage.2018.03.049
- 408 Huijbers, W., Van Dijk, K. R. A., Boenniger, M. M., Stirnberg, R., & Breteler, M. M. B.
409 (2017). Less head motion during MRI under task than resting-state conditions.
410 *NeuroImage*, 147, 111–120. doi: 10.1016/j.neuroimage.2016.12.002
- 411 Knight, M. J., McCann, B., Tsivos, D., Couthard, E., & Kauppinen, R. A. (2016).
412 Quantitative t1 and t2 MRI signal characteristics in the human brain: different
413 patterns of MR contrasts in normal ageing. *Magnetic Resonance Materials in*
414 *Physics, Biology and Medicine*, 29, 833–842. doi: 10.1007/s10334-016-0573-0
- 415 Maclaren, J., Herbst, M., Speck, O., & Zaitsev, M. (2013). Prospective motion correction
416 in brain imaging: A review. *Magnetic Resonance in Medicine*, 69, 621–636. doi:
417 10.1002/mrm.24314
- 418 Madan, C. R. (2017). Advances in studying brain morphology: The benefits of
419 open-access data. *Frontiers in Human Neuroscience*, 11, 405. doi:
420 10.3389/fnhum.2017.00405
- 421 Madan, C. R. (2018). Shape-related characteristics of age-related differences in
422 subcortical structures. *Aging & Mental Health*. doi:
423 10.1080/13607863.2017.1421613
- 424 Madan, C. R., & Kensinger, E. A. (2016). Cortical complexity as a measure of
425 age-related brain atrophy. *NeuroImage*, 134, 617–629. doi:
426 10.1016/j.neuroimage.2016.04.029
- 427 Madan, C. R., & Kensinger, E. A. (2017a). Age-related differences in the structural
428 complexity of subcortical and ventricular structures. *Neurobiology of Aging*, 50,
429 87–95. doi: 10.1016/j.neurobiolaging.2016.10.023
- 430 Madan, C. R., & Kensinger, E. A. (2017b). Test–retest reliability of brain morphology

- 431 estimates. *Brain Informatics*, 4, 107–121. doi: 10.1007/s40708-016-0060-4
- 432 Madan, C. R., & Kensinger, E. A. (2018). Predicting age from cortical structure across
433 the lifespan. *European Journal of Neuroscience*, 47, 399–416. doi: 10.1111/ejn.13835
- 434 Magnaldi, S., Ukmar, M., Vasciaveo, A., Longo, R., & Pozzi-Mucelli, R. (1993). Contrast
435 between white and grey matter: MRI appearance with ageing. *European Radiology*,
436 3. doi: 10.1007/bf00169600
- 437 Marcus, D. S., Harms, M. P., Snyder, A. Z., Jenkinson, M., Wilson, J. A., Glasser, M. F., ...
438 Essen, D. C. V. (2013). Human Connectome Project informatics: Quality control,
439 database services, and data visualization. *NeuroImage*, 80, 202–219. doi:
440 10.1016/j.neuroimage.2013.05.077
- 441 McKay, D. R., Knowles, E. E. M., Winkler, A. A. M., Sprooten, E., Kochunov, P., Olvera,
442 R. L., ... Glahn, D. C. (2014). Influence of age, sex and genetic factors on the
443 human brain. *Brain Imaging and Behavior*, 8, 143–152. doi:
444 10.1007/s11682-013-9277-5
- 445 Overmeyer, S. (1996). Angstverarbeitung von psychisch auffälligen Kindern im
446 Kernspintomogramm. *Monatsschrift Kinderheilkunde*, 144, 1337–1341. doi:
447 10.1007/s001120050091
- 448 Pardoe, H. R., Hiess, R. K., & Kuzniecky, R. (2016). Motion and morphometry in
449 clinical and nonclinical populations. *NeuroImage*, 135, 177–185. doi:
450 10.1016/j.neuroimage.2016.05.005
- 451 Pliszka, S. R., Lancaster, J., Liotti, M., & Semrud-Clikeman, M. (2006). Volumetric MRI
452 differences in treatment-naive vs chronically treated children with ADHD.
453 *Neurology*, 67, 1023–1027. doi: 10.1212/01.wnl.0000237385.84037.3c
- 454 Power, J. D., Barnes, K. A., Snyder, A. Z., Schlaggar, B. L., & Petersen, S. E. (2012).
455 Spurious but systematic correlations in functional connectivity MRI networks
456 arise from subject motion. *NeuroImage*, 59, 2142–2154. doi:
457 10.1016/j.neuroimage.2011.10.018
- 458 Raschle, N. M., Lee, M., Buechler, R., Christodoulou, J. A., Chang, M., Vakil, M., ...
459 Gaab, N. (2009). Making MR imaging child's play - pediatric neuroimaging

- 460 protocol, guidelines and procedure. *Journal of Visualized Experiments*. doi:
461 10.3791/1309
- 462 Reuter, M., Tisdall, M. D., Qureshi, A., Buckner, R. L., van der Kouwe, A. J., & Fischl, B.
463 (2015). Head motion during MRI acquisition reduces gray matter volume and
464 thickness estimates. *NeuroImage*, *107*, 107–115. doi:
465 10.1016/j.neuroimage.2014.12.006
- 466 Romero-Corral, A., Somers, V. K., Sierra-Johnson, J., Thomas, R. J., Collazo-Clavell,
467 M. L., Korinek, J., ... Lopez-Jimenez, F. (2008). Accuracy of body mass index in
468 diagnosing obesity in the adult general population. *International Journal of Obesity*,
469 *32*, 959–966. doi: 10.1038/ijo.2008.11
- 470 Ronan, L., Alexander-Bloch, A. F., Wagstyl, K., Farooqi, S., Brayne, C., Tyler, L. K., &
471 Fletcher, P. C. (2016). Obesity associated with increased brain age from midlife.
472 *Neurobiology of Aging*, *47*, 63–70. doi: 10.1016/j.neurobiolaging.2016.07.010
- 473 Salat, D. H., Buckner, R. L., Snyder, A. Z., Greve, D. N., Desikan, R. S. R., Busa, E., ...
474 Fischl, B. (2004). Thinning of the cerebral cortex in aging. *Cerebral Cortex*, *14*,
475 721–730. doi: 10.1093/cercor/bhh032
- 476 Salat, D. H., Lee, S. Y., van der Kouwe, A. J., Greve, D. N., Fischl, B., & Rosas, H. D.
477 (2009). Age-associated alterations in cortical gray and white matter signal
478 intensity and gray to white matter contrast. *NeuroImage*, *48*, 21–28. doi:
479 10.1016/j.neuroimage.2009.06.074
- 480 Savalia, N. K., Agres, P. F., Chan, M. Y., Feczko, E. J., Kennedy, K. M., & Wig, G. S.
481 (2017). Motion-related artifacts in structural brain images revealed with
482 independent estimates of in-scanner head motion. *Human Brain Mapping*, *38*,
483 472–492. doi: 10.1002/hbm.23397
- 484 Schaer, M., Cuadra, M. B., Schmansky, N., Fischl, B., Thiran, J.-P., & Eliez, S. (2012).
485 How to measure cortical folding from MR images: A step-by-step tutorial to
486 compute local gyrification index. *Journal of Visualized Experiments*, e3417. doi:
487 10.3791/3417
- 488 Schwarz, G. (1978). Estimating the dimension of a model. *Annals of Statistics*, *6*,

- 489 461–464. doi: 10.1214/aos/1176344136
- 490 Shafto, M. A., Tyler, L. K., Dixon, M., Taylor, J. R., Rowe, J. B., ... Matthews, F. E.
491 (2014). The Cambridge Centre for Ageing and Neuroscience (Cam-CAN) study
492 protocol: a cross-sectional, lifespan, multidisciplinary examination of healthy
493 cognitive ageing. *BMC Neurology*, 14, 204. doi: 10.1186/s12883-014-0204-1
- 494 Shaw, M. E., Abhayaratna, W. P., Anstey, K. J., & Cherbuin, N. (2017). Increasing body
495 mass index at midlife is associated with increased cortical thinning in alzheimer's
496 disease-vulnerable regions. *Journal of Alzheimer's Disease*, 59, 113–120. doi:
497 10.3233/JAD-170055
- 498 Shaw, M. E., Sachdev, P. S., Abhayaratna, W., Anstey, K. J., & Cherbuin, N. (2018, oct).
499 Body mass index is associated with cortical thinning with different patterns in
500 mid- and late-life. *International Journal of Obesity*, 42(3), 455–461. doi:
501 10.1038/ijo.2017.254
- 502 Stucht, D., Danishad, K. A., Schulze, P., Godenschweger, F., Zaitsev, M., & Speck, O.
503 (2015). Highest resolution in vivo human brain MRI using prospective motion
504 correction. *PLOS ONE*, 10, e0133921. doi: 10.1371/journal.pone.0133921
- 505 Tambini, A., & Davachi, L. (2013). Persistence of hippocampal multivoxel patterns into
506 postencoding rest is related to memory. *Proceedings of the National Academy of
507 Sciences USA*, 110, 19591–19596. doi: 10.1073/pnas.1308499110
- 508 Taylor, J. R., Williams, N., Cusack, R., Auer, T., Shafto, M. A., Dixon, M., ... Henson,
509 R. N. (2017). The Cambridge Centre for Ageing and Neuroscience (Cam-CAN)
510 data repository: Structural and functional MRI, MEG, and cognitive data from a
511 cross-sectional adult lifespan sample. *NeuroImage*, 144, 262–269. doi:
512 10.1016/j.neuroimage.2015.09.018
- 513 Theys, C., Wouters, J., & Ghesquière, P. (2014). Diffusion tensor imaging and
514 resting-state functional MRI-scanning in 5- and 6-year-old children: Training
515 protocol and motion assessment. *PLOS ONE*, 9, e94019. doi:
516 10.1371/journal.pone.0094019
- 517 Tisdall, M. D., Reuter, M., Qureshi, A., Buckner, R. L., Fischl, B., & van der Kouwe, A. J.

- 518 (2016). Prospective motion correction with volumetric navigators (vNavs)
519 reduces the bias and variance in brain morphometry induced by subject motion.
520 *NeuroImage*, 127, 11–22. doi: 10.1016/j.neuroimage.2015.11.054
- 521 van Kesteren, M. T. R., Fernandez, G., Norris, D. G., & Hermans, E. J. (2010). Persistent
522 schema-dependent hippocampal-neocortical connectivity during memory
523 encoding and postencoding rest in humans. *Proceedings of the National Academy of
524 Sciences USA*, 107, 7550–7555. doi: 10.1073/pnas.0914892107
- 525 Vanderwal, T., Kelly, C., Eilbott, J., Mayes, L. C., & Castellanos, F. X. (2015). Inscapes :
526 A movie paradigm to improve compliance in functional magnetic resonance
527 imaging. *NeuroImage*, 122, 222–232. doi: 10.1016/j.neuroimage.2015.07.069
- 528 Veit, R., Kullmann, S., Heni, M., Machann, J., Häring, H.-U., Fritsche, A., & Preissl, H.
529 (2014). Reduced cortical thickness associated with visceral fat and BMI.
530 *NeuroImage: Clinical*, 6, 307–311. doi: 10.1016/j.nicl.2014.09.013
- 531 von Rhein, D., Mennes, M., van Ewijk, H., Groenman, A. P., Zwiers, M. P., Oosterlaan,
532 J., ... Buitelaar, J. (2015). The NeuroIMAGE study: a prospective phenotypic,
533 cognitive, genetic and MRI study in children with attention-deficit/hyperactivity
534 disorder. design and descriptives. *European Child & Adolescent Psychiatry*, 24,
535 265–281. doi: 10.1007/s00787-014-0573-4
- 536 Wu Nordahl, C., Simon, T. J., Zierhut, C., Solomon, M., Rogers, S. J., & Amaral, D. G.
537 (2008). Methods for acquiring structural MRI data in very young children with
538 autism without the use of sedation. *Journal of Autism and Developmental Disorders*,
539 38, 1581–1590. doi: 10.1007/s10803-007-0514-x
- 540 Wylie, G. R., Genova, H., DeLuca, J., Chiaravalloti, N., & Sumowski, J. F. (2014).
541 Functional magnetic resonance imaging movers and shakers: Does
542 subject-movement cause sampling bias? *Human Brain Mapping*, 35, 1–13. doi:
543 10.1002/hbm.22150
- 544 Yuan, W., Altaye, M., Ret, J., Schmithorst, V., Byars, A. W., Plante, E., & Holland, S. K.
545 (2009). Quantification of head motion in children during various fMRI language
546 tasks. *Human Brain Mapping*, 30, 1481–1489. doi: 10.1002/hbm.20616

- 547 Zacà, D., Hasson, U., Minati, L., & Jovicich, J. (in press). Method for retrospective
548 estimation of natural head movement during structural MRI. *Journal of Magnetic*
549 *Resonance Imaging*. doi: 10.1002/jmri.25959
- 550 Zeng, L.-L., Wang, D., Fox, M. D., Sabuncu, M., Hu, D., Ge, M., . . . Liu, H. (2014).
551 Neurobiological basis of head motion in brain imaging. *Proceedings of the National*
552 *Academy of Sciences USA*, 111, 6058–6062. doi: 10.1073/pnas.1317424111